

Optical injection of mammalian cells using a microfluidic platform

Robert F. Marchington,^{1,*} Yoshihiko Arita,¹ Xanthi Tsampoula,¹
Frank J. Gunn-Moore,² and Kishan Dholakia¹

¹SUPA, School of Physics & Astronomy, University of St Andrews, St. Andrews, Fife, KY16 9SS, UK

²School of Biology, University of St Andrews, St. Andrews, Fife, KY16 9TS, UK

*rm346@st-andrews.ac.uk

Abstract: The use of a focused laser beam to create a sub-micron hole in the plasma membrane of a cell (photoporation), for the selective introduction of membrane impermeable substances (optical injection) including nucleic acids (optical transfection), is a powerful technique most commonly applied to treat single cells. However, particularly for femtosecond photoporation, these studies have been limited to low throughput, small-scale studies, because they require sequential dosing of individual cells. Herein, we describe a microfluidic photoporation system for increased throughput and automated optical injection of cells. Hydrodynamic focusing is employed to direct a flow of single-file cells through a focused femtosecond laser beam for photoporation. Upon traversing the beam, a number of transient pores potentially open across the extracellular membrane, which allows the uptake of the surrounding fluid media into the cytoplasm, also containing the chosen injection agent. The process is entirely automated and a rate of 1 cell/sec could readily be obtained, enabling several thousand cells to be injected per hour using this system. The efficiency of optically injecting propidium iodide into HEK293 mammalian cells was found to be $42 \pm 8\%$, or $28 \pm 4\%$ taking into account the requirement of post-injection viability, as tested using Calcein AM. This work now opens the way for combining photoporation with microfluidic analyses, sorting, purification or on-chip cell culture studies.

©2010 Optical Society of America

OCIS codes: (000.1430) Biology and medicine; (020.4180) Multiphoton processes; (140.3538) Lasers, pulsed; (140.7090) Ultrafast lasers; (170.3890) Medical optics instrumentation; (170.7160) Ultrafast technology.

References and links

1. M. Tsukakoshi, S. Kurata, Y. Nomiya, Y. Ikawa, and T. Kasuya, "A novel method of DNA transfection by laser microbeam cell surgery," *Appl. Phys. B* **35**(3), 135–140 (1984).
2. L. Paterson, B. Agate, M. Comrie, R. Ferguson, T. K. Lake, J. E. Morris, A. E. Carruthers, C. T. A. Brown, W. Sibbett, P. E. Bryant, F. Gunn-Moore, A. C. Riches, and K. Dholakia, "Photoporation and cell transfection using a violet diode laser," *Opt. Express* **13**(2), 595–600 (2005).
3. M. L. Torres-Mapa, L. Angus, M. Ploschner, K. Dholakia, and F. J. Gunn-Moore, "Transient transfection of mammalian cells using a violet diode laser," *J. Biomed. Opt.* **15**(4), 041506 (2010).
4. H. Schneckenburger, A. Hendinger, R. Saifer, W. S. L. Strauss, and M. Schmitt, "Laser-assisted optoporation of single cells," *J. Biomed. Opt.* **7**(3), 410–416 (2002).
5. A. V. Nikolskaya, V. P. Nikolski, and I. R. Efimov, "Gene printer: laser-scanning targeted transfection of cultured cardiac neonatal rat cells," *Cell Commun. Adhes.* **13**(4), 217–222 (2006).
6. G. Palumbo, M. Caruso, E. Crescenzi, M. F. Tecce, G. Roberti, and A. Colasanti, "Targeted gene transfer in eucaryotic cells by dye-assisted laser optoporation," *J. Photochem. Photobiol. B* **36**(1), 41–46 (1996).
7. I. B. Clark, E. G. Hanania, J. Stevens, M. Gallina, A. Fieck, R. Brandes, B. O. Palsson, and M. R. Koller, "Optoinjection for efficient targeted delivery of a broad range of compounds and macromolecules into diverse cell types," *J. Biomed. Opt.* **11**(1), 014034 (2006).
8. T. Knoll, L. Trojan, S. Langbein, S. Sagi, P. Alken, and M. S. Michel, "Impact of holmium:YAG and neodymium:YAG lasers on the efficacy of DNA delivery in transitional cell carcinoma," *Lasers Med. Sci.* **19**(1), 33–36 (2004).

9. H. Schinkel, P. Jacobs, S. Schillberg, and M. Wehner, "Infrared picosecond laser for perforation of single plant cells," *Biotechnol. Bioeng.* **99**(1), 244–248 (2008).
10. C. T. A. Brown, D. J. Stevenson, X. Tsampoula, C. McDougall, A. A. Lagatsky, W. Sibbett, F. J. Gunn-Moore, and K. Dholakia, "Enhanced operation of femtosecond lasers and applications in cell transfection," *J. Biophotonics* **1**(3), 183–199 (2008).
11. L. E. Barrett, J. Y. Sul, H. Takano, E. J. Van Bockstaele, P. G. Haydon, and J. H. Eberwine, "Region-directed phototransfection reveals the functional significance of a dendritically synthesized transcription factor," *Nat. Methods* **3**(6), 455–460 (2006).
12. M. Lei, H. Xu, H. Yang, and B. Yao, "Femtosecond laser-assisted microinjection into living neurons," *J. Neurosci. Methods* **174**(2), 215–218 (2008).
13. P. Mthunzi, K. Dholakia, and F. Gunn-Moore, "Photo-transfection of mammalian cells using femtosecond laser pulses: optimisation and applicability to stem cell differentiation," *J. Biomed. Opt.* **15**(4), 041507 (2010).
14. C. Peng, R. E. Palazzo, and I. Wilke, "Laser intensity dependence of femtosecond near-infrared optoinjection," *Phys. Rev. E Stat. Nonlin. Soft Matter Phys.* **75**(4), 041903 (2007).
15. D. Stevenson, B. Agate, X. Tsampoula, P. Fischer, C. T. A. Brown, W. Sibbett, A. Riches, F. Gunn-Moore, and K. Dholakia, "Femtosecond optical transfection of cells: viability and efficiency," *Opt. Express* **14**(16), 7125–7133 (2006).
16. U. K. Tirlapur, and K. König, "Targeted transfection by femtosecond laser," *Nature* **418**(6895), 290–291 (2002).
17. X. Tsampoula, V. Garces-Chavez, M. Comrie, D. J. Stevenson, B. Agate, C. T. A. Brown, F. Gunn-Moore, and K. Dholakia, "Femtosecond cellular transfection using a nondiffracting light beam," *Appl. Phys. Lett.* **91**(5), 053902–053903 (2007).
18. A. Uchugonova, K. König, R. Rueckle, A. Iseemann, and G. Tempea, "Targeted transfection of stem cells with sub-20 femtosecond laser pulses," *Opt. Express* **16**(13), 9357–9364 (2008).
19. A. Yamaguchi, Y. Hosokawa, G. Louit, T. Asahi, C. Shukunami, Y. Hiraki, and H. Masuhara, "Nanoparticle injection to single animal cells using femtosecond laser-induced impulsive force," *Adv. Mater.* **93**, 39–43 (2008).
20. E. Zeira, A. Manevitch, A. Khatchatourians, O. Pappo, E. Hyam, M. Darash-Yahana, E. Tavor, A. Honigman, A. Lewis, and E. Galun, "Femtosecond infrared laser—an efficient and safe in vivo gene delivery system for prolonged expression," *Mol. Ther.* **8**(2), 342–350 (2003).
21. C. McDougall, D. J. Stevenson, C. T. A. Brown, F. Gunn-Moore, and K. Dholakia, "Targeted optical injection of gold nanoparticles into single mammalian cells," *J Biophotonics* **2**(12), 736–743 (2009).
22. J. Baumgart, W. Bintig, A. Ngezahayo, S. Willenbrock, H. Murua Escobar, W. Ertmer, H. Lubatschowski, and A. Heisterkamp, "Quantified femtosecond laser based opto-perforation of living GFSHR-17 and MTH53 a cells," *Opt. Express* **16**(5), 3021–3031 (2008).
23. X. Tsampoula, K. Taguchi, T. Cizmár, V. Garces-Chavez, N. Ma, S. Mohanty, K. Mohanty, F. Gunn-Moore, and K. Dholakia, "Fibre based cellular transfection," *Opt. Express* **16**(21), 17007–17013 (2008).
24. S. Sagi, T. Knoll, L. Trojan, A. Schaaf, P. Alken, and M. S. Michel, "Gene delivery into prostate cancer cells by holmium laser application," *Prostate Cancer Prostatic Dis.* **6**(2), 127–130 (2003).
25. D. J. Stevenson, F. J. Gunn-Moore, P. Campbell, and K. Dholakia, "The Handbook of Photonics for Medical Science," 1 ed., V. V. Tuchin, ed. (CRC Press, USA, 2010), pp. 87–117.
26. A. Vogel, N. Linz, S. Freidank, and G. U. Paltauf, "Femtosecond-laser-induced nanocavitation in water: implications for optical breakdown threshold and cell surgery," *Phys. Rev. Lett.* **100**(3), 038102 (2008).
27. T. Cižmár, V. Kollárová, X. Tsampoula, F. Gunn-Moore, W. Sibbett, Z. Bouchal, and K. Dholakia, "Generation of multiple Bessel beams for a biophotonics workstation," *Opt. Express* **16**(18), 14024–14035 (2008).
28. A. Noori, P. R. Selvaganapathy, and J. Wilson, "Microinjection in a microfluidic format using flexible and compliant channels and electroosmotic dosage control," *Lab Chip* **9**(22), 3202–3211 (2009).
29. A. Adamo, and K. F. Jensen, "Microfluidic based single cell microinjection," *Lab Chip* **8**(8), 1258–1261 (2008).
30. N. Bao, Y. Zhan, and C. Lu, "Microfluidic electroporative flow cytometry for studying single-cell biomechanics," *Anal. Chem.* **80**(20), 7714–7719 (2008).
31. J. Wang, M. J. Stine, and C. Lu, "Microfluidic cell electroporation using a mechanical valve," *Anal. Chem.* **79**(24), 9584–9587 (2007).
32. Y. Zhan, J. Wang, N. Bao, and C. Lu, "Electroporation of cells in microfluidic droplets," *Anal. Chem.* **81**(5), 2027–2031 (2009).
33. T. Zhu, C. Luo, J. Huang, C. Xiong, Q. Ouyang, and J. Fang, "Electroporation based on hydrodynamic focusing of microfluidics with low dc voltage," *Biomed. Microdevices* **12**(1), 35–40 (2010).
34. R. Ziv, Y. Steinhardt, G. Pelled, D. Gazit, and B. Rubinsky, "Micro-electroporation of mesenchymal stem cells with alternating electrical current pulses," *Biomed. Microdevices* **11**(1), 95–101 (2009).
35. E. Neumann, M. Schaefer-Ridder, Y. Wang, and P. H. Hofschneider, "Gene transfer into mouse lymphoma cells by electroporation in high electric fields," *EMBO J.* **1**(7), 841–845 (1982).
36. J. A. Wolff, R. W. Malone, P. Williams, W. Chong, G. Acsadi, A. Jani, and P. L. Felgner, "Direct gene transfer into mouse muscle in vivo," *Science* **247**(4949), 1465–1468 (1990).
37. N. S. Yang, J. Burkholder, B. Roberts, B. Martinell, and D. McCabe, "In vivo and in vitro gene transfer to mammalian somatic cells by particle bombardment," *Proc. Natl. Acad. Sci. U.S.A.* **87**(24), 9568–9572 (1990).
38. P. L. Felgner, T. R. Gadek, M. Holm, R. Roman, H. W. Chan, M. Wenz, J. P. Northrop, G. M. Ringold, and M. Danielsen, "Lipofection: a highly efficient, lipid-mediated DNA-transfection procedure," *Proc. Natl. Acad. Sci. U.S.A.* **84**(21), 7413–7417 (1987).
39. K. L. Douglas, "Toward development of artificial viruses for gene therapy: a comparative evaluation of viral and non-viral transfection," *Biotechnol. Prog.* **24**(4), 871–883 (2008).

40. M. M. Wang, E. Tu, D. E. Raymond, J. M. Yang, H. Zhang, N. Hagen, B. Dees, E. M. Mercer, A. H. Forster, I. Kariv, P. J. Marchand, and W. F. Butler, "Microfluidic sorting of mammalian cells by optical force switching," *Nat. Biotechnol.* **23**(1), 83–87 (2005).
41. A. Y. Lau, L. P. Lee, and J. W. Chan, "An integrated optofluidic platform for Raman-activated cell sorting," *Lab Chip* **8**(7), 1116–1120 (2008).
42. R. F. Marchington, M. Mazilu, S. Kuriakose, V. Garcés-Chávez, P. J. Reece, T. F. Krauss, M. Gu, and K. Dholakia, "Optical deflection and sorting of microparticles in a near-field optical geometry," *Opt. Express* **16**(6), 3712–3726 (2008).
43. K. Dholakia, W. M. Lee, L. Paterson, M. P. Macdonald, R. McDonald, I. Andreev, P. Mthunzi, C. T. A. Brown, R. F. Marchington, and A. C. Riches, "Optical separation of cells on potential energy landscapes: enhancement with dielectric tagging," *IEEE J. Sel. Top. Quantum Electron.* **13**(6), 1646–1654 (2007).
44. J. C. McDonald, and G. M. Whitesides, "Poly(dimethylsiloxane) as a material for fabricating microfluidic devices," *Acc. Chem. Res.* **35**(7), 491–499 (2002).
45. K. Haubert, T. Drier, and D. Beebe, "PDMS bonding by means of a portable, low-cost corona system," *Lab Chip* **6**(12), 1548–1549 (2006).
46. G.-B. Lee, C.-C. Chang, S.-B. Huang, and R.-J. Yang, "The hydrodynamic focusing effect inside rectangular microchannels," *J. Micromech. Microeng.* **16**(5), 1024–1032 (2006).
47. C. M. Pitsillides, E. K. Joe, X. Wei, R. R. Anderson, and C. P. Lin, "Selective cell targeting with light-absorbing microparticles and nanoparticles," *Biophys. J.* **84**(6), 4023–4032 (2003).
48. W. M. Lee, P. J. Reece, R. F. Marchington, N. K. Metzger, and K. Dholakia, "Construction and calibration of an optical trap on a fluorescence optical microscope," *Nat. Protoc.* **2**(12), 3226–3238 (2007).
49. P. B. Howell, Jr., J. P. Golden, L. R. Hilliard, J. S. Erickson, D. R. Mott, and F. S. Ligler, "Two simple and rugged designs for creating microfluidic sheath flow," *Lab Chip* **8**(7), 1097–1103 (2008).

1. Introduction

Optical injection is a promising technique for transiently perforating the membrane of living biological cells, using a tightly focused laser beam to allow impermeable molecules, such as drugs, dyes or nucleic acids (including plasmid DNA), to pass into the cytoplasm. First demonstrated by Tsukakoshi *et al.* in 1984 [1], a wide spectrum of laser sources have since been successfully implemented, including continuous wave (CW) at 405 nm [2,3] and 488 nm [4–6] as well as pulsed laser sources of nano-, pico- [1,7–9] and most notably of femtosecond (fs) pulse durations in the near infrared [10–23], and at 2080 nm (Ho:YAG) [8,24]. Femtosecond optical injection is a non-invasive and sterile technique, with recent studies in delivering plasmid DNA for subsequent transfection of the cells with efficiencies of up to 80% [13] and demonstrating excellent cell viability. Optical transfection has been demonstrated on a wide range of biological cells, both plant [9] and animal cells, including mammalian neurons [11] and stem cells [13,18]. Indeed, it has recently been reported that optical injection can be utilized to differentiate mouse embryonic stem cell colonies into the extraembryonic endoderm [13].

Nano- and picosecond optical injection can be used to treat many dozens of cells simultaneously [1,7–9], but is associated with a large "zone of destruction," with viable cell permeation only occurring on the periphery of a laser-induced acoustic shockwave [25]. Femtosecond and CW sources facilitate the treatment of single cells, resulting in improved efficiency and viability. The most widely used laser source is the Kerr lens mode-locked fs Titanium:Sapphire laser, which when focused through a high numerical aperture lens will produce a sub-micron diffraction-limited laser spot, with peak powers of the order of KW's at the focus. When delivered to the cell membrane, this will generate multi-photon absorption and ionization that forms a low-density free-electron plasma within the lipid bilayer [26]. The transient interaction invokes the cell to uptake femtoliter volumes of the extra-cellular fluid, containing the nanoparticles [21], charged molecules (such as DNA) or other reagents for insertion into the cell. Importantly, the power levels used are below the threshold for optical breakdown [26]; thus minimizing collateral damage and maintaining the viability of the cell. Cells are targeted one at a time and as such femtosecond optical injection is an excellent tool for single cell analysis, or for porating small populations of a few tens of cells.

However, the ability to localize the photoporation effect to a precise region on a single cell has been both advantageous and limiting. Whilst this methodology is suitable for single cell analysis, dosing more than ~100 cells is time consuming. This limitation has prohibited larger studies on cell populations. One method for improving the throughput of fs optical injection is

to remove the necessity for manually locating the beam focus on each cell. This has previously been achieved using a spatial light modulator (SLM) to produce a “diffraction-free” Bessel beam, controlled by a “point and click” interface, allowing a user to select cells at will on the screen for injection, without the need for careful positioning of the beam focus [27]. The method addressed in this work is to introduce a cell delivery method that streams continually cells through the beam for automated injection. Indeed, this has previously been demonstrated by making use of microfluidic systems combined with microinjection [28,29] and electroporation [30–34].

In this study, we report a significant step towards high cell throughputs and automated optical injection by making use of microfluidic cell delivery which we demonstrate on a mammalian cell line. The precision of focused femtosecond pulses was combined with hydrodynamic focusing, to produce a single-file flow of cells through the laser beam for optical injection. The injection efficiency and viability of this new system was determined using propidium iodide (PI) dye and calcein AM (CAM) respectively, and was found to be on par with ‘static’ fs photoporation studies of adherent cells. Flow rates of one cell per second could readily be obtained, enabling several thousand viable injected cells to be produced in an hour. This work indicates optical injection as a favorable alternative to other techniques such as electroporation [35], microinjection [36], ballistic methods [37], lipofection [38] or viral [39] mediated transfection. The combination of microfluidic photoporation with on-chip sample mixing, cell culture or analysis or alternatively microfluidic sorting schemes, such as fluorescence/Raman activated cell sorting (FACS/RACS [40,41]) or passive optical sorting [42,43] can now all be envisaged.

2. Microfluidic chip and setup

The microfluidic chips for this study were fabricated in poly-dimethylsiloxane (PDMS) using standard soft lithography procedures [44]. The PDMS chip was designed to have an inlet and outlet port for the insertion and collection of cells, and a hydrodynamic focusing region to force the cell sample into a thin (sub-cell sized) stream down the center of the fluidic channel thereby directing all cells through the photoporation beam. Briefly the fluidic design was composed in a CAD software package and printed to high resolution transparency (Circuit Graphics Ltd). Photolithography was used to form a mold in 70 μm thick SU-8 (Microchem) resist on a silicon wafer and silanized with perfluorooctyltrichlorosilane (S13125, Flurochem). Two-part PDMS (Sylgard 184, Dow Corning) was mixed in a 1:10 weight ratio, degassed, poured on to the mold and baked at 65°C for two hours. The channel dimensions were 150 μm wide by 70 μm high throughout except at the reservoirs that were 3 mm in diameter.

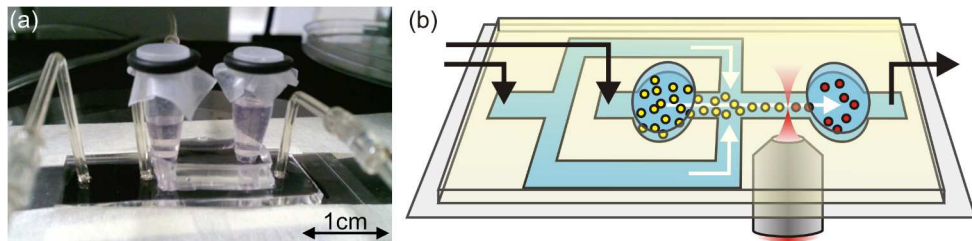


Fig. 1. (a) Image of the PDMS chip showing micro-centrifuge tubes for cell insertion and collection, and the two inlet pipes on the left for buffer and sample flow and a single outlet pipe on the right. (b) Microfluidic channel layout on the PDMS chip (not to scale). The cells are first inserted directly into chip via an adapted micro-centrifuge tube (left-most). The three syringe pumps then drive the fluid as indicated by the arrows. Cells pass into the hydrodynamic focusing junction, forcing them to flow one at a time through the femtosecond laser beam (as focused into the chip via the objective lens), where optical injection occurs. The beam is positioned approximately 300 μm downstream of the hydrodynamic focusing junction. Cells come to rest under the second micro-centrifuge tube, ready for collection with a pipette for culture and/or analysis.

To incorporate cell injection and collection ports, it was necessary to define a second section of PDMS on top of the first to provide sufficient support for the cell ports, as can be observed in Fig. 1. Once cured the PDMS was peeled from the mold, inlets punched (Harris Micropunch) and irreversibly sealed to a type-1 coverslip (VWR International) using a hand-held plasma treater [45]. The inlet sizes were 1.2 mm and 3 mm for the pipes and 0.5 ml micro-centrifugation tubes respectively. Adapted 0.5 ml micro-centrifugation tubes (cap and base removed) were later inserted into the punched holes to act as cell injection and collection reservoirs.

Several features were incorporated into the fluidic setup to minimize fluctuations in the fluid flow in order to obtain a steady and reproducible flow of cells over the course of the experiment. Three syringe pumps (Harvard Apparatus, Pico Plus) were used in a “push-pull” configuration to generate stable hydrodynamic focusing: one to drive the sample stream, one for the buffer streams and a third as a suction pump on the outlet. Rigid Radel R (Upchurch) tubing was used to interface the chip to the syringe pumps (see Fig. 2), providing significantly more stable flow than the Tygon R3603 flexible tubing, that was used purely for interfacing the peristaltic pump. Four-way L-junction switching valves (Upchurch) were used to connect the peristaltic and syringe pump fluid lines, allowing the chip and pipes to be flushed and filled as desired using the peristaltic pump, but also isolated to just the syringe pump lines when running the experiment. Gastight (Hamilton) 100 μl syringes were used with the syringe pumps.

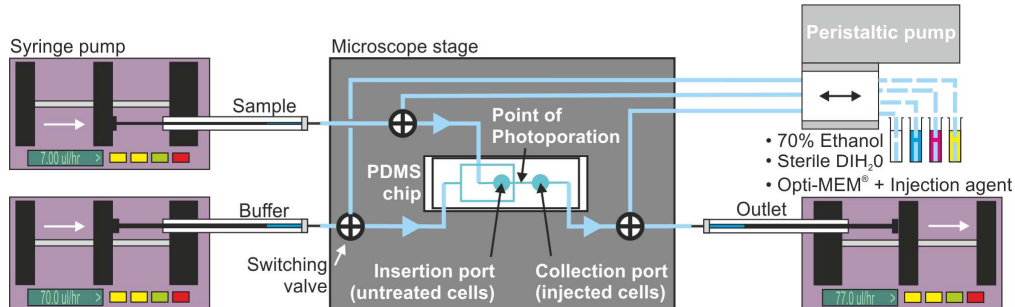


Fig. 2. Fluidic setup required for cleaning, sterilizing and flowing cells. Cleaning, sterilizing and filling of the fluidics with cell medium is conducted using the peristaltic pump. Syringe pumps are used for flowing of the cells for optical injection, and operate in a “push-pull” configuration to obtain stable fluid flow. Layout of the PDMS microfluidic chip is also shown, which matches with Fig. 1. The injection agent is added the Opti-MEM® before filling the chip and piping at the start of the experiment.

The ratio of the sample to buffer flow determines the hydrodynamic focusing ratio and for a channel width of 150 μm , a 1:5 ratio gives 13%, or 20 μm which is approximately one cell width [46]. Flow rates were controlled via a Labview interface and set to 7 μlhr^{-1} and 70 μlhr^{-1} for sample and buffer pumps respectively. Depending on the confluence of the cell sample, this gave a rate of 1 cell per second, and a cell velocity of $1100 \pm 100 \mu\text{ms}^{-1}$. It should be noted that the velocity of the cells is lower than the peak fluid velocity in the channel, because the cells were situated in the lower half of the channel due to gravity. As the cells are denser than the fluid medium, this allows them to rest on the bottom of the injection reservoir at the start of the experiment. At the start of an experiment, there will be some lift of the cells due to Bernoulli lift in a parabolic flow profile, but at these flow rates it was not expected to contribute to an elevation of even 10 μm from the channel base. The clearest brightfield image of cells, as they traversed the laser spot, was at a position of 6 μm above the coverslip. The cells were observed to flow at similar velocities, indicating similar positions in a parabolic shaped flow profile. The flow rates used throughout were first determined empirically to provide single file flow of cells at the required velocity of $1100 \mu\text{ms}^{-1}$.

3. Cell culture, preparation and collection

Propidium iodide (PI, Sigma-Aldrich) is a membrane impermeable stain commonly used in proof of principle cell injection studies. PI is only taken up by cells whose membranes have been compromised and will be excluded by living viable cells. It interacts with the DNA of the host cell by binding to specific nucleotides within the DNA strand. Once the binding occurs, and under the right excitation illumination, the PI molecules will exhibit intense fluorescence at 617 nm. In order to verify PI uptake and confirm cell viability, upon treatment, the cells were stained with the membrane permeable neutral vital dye Calcein-AM (CAM, Invitrogen), which is rapidly converted by cell esterases into calcein that fluoresces at 530 nm within a viable cell [47]. These two fluorescent dyes therefore work well in conjunction to identify viable and successfully optically injected cells.

Human embryonic kidney (HEK293) cells were cultured in Dulbecco's Modified Eagle's Medium (DMEM, Sigma-Aldrich) with 10% fetal calf serum (FCS, Globepharm), 20 μgml^{-1} streptomycin (Sigma-Aldrich) and 20 μgml^{-1} penicillin (Sigma-Aldrich) in T25 flasks (Fisher Scientific) kept at 37°C and 5% CO₂ in an incubator. The cell population was expanded and brought to sub-confluence nominally three times per week using Trypsin-EDTA (Sigma-Aldrich). The process of trypsinising the cell stock defines the cell passage number, which throughout the experiments was kept between 15 and 30.

For the purposes of the experiment, HEK293 cells cultured in a T25 flask were suspended by adding 1 ml of Trypsin-EDTA and centrifuged at 0.2 g for 5 minutes in a micro-centrifuge tube (1.5 ml). The Trypsin was carefully removed from the medium and cells were rinsed twice with filtered Opti-MEM® to remove residual Trypsin. Next, the cells were gently stirred in 1 ml of fresh filtered Opti-MEM® with 1.5 μM of the injection agent PI, and passed through a 40 μm filter (BD Falcon Cell Strainer, VWR) to remove any clumps of adhered cells. Finally, 200 μl of this cell suspension medium was aliquoted into a micro-centrifuge tube, and 20 μl of this was loaded into the microfluidic chip for an experiment.

The fluid medium used for filling the microfluidic chip and associated piping was also prepared immediately prior to the experiment. 3 ml of filtered Opti-MEM® in a T25 flask with a gas permeable cap was degassed by a vacuum pump for 10 minutes, which prevented the formation of gas bubbles within the microfluidic chip during experiments. 3 μl of 1 mgml^{-1} water solution of PI was loaded into the flask to obtain a final PI concentration of 1.5 μM in degassed Opti-MEM®.

4. Optical setup

The optical setup is shown in Fig. 3. A mode-locked Titanium:Sapphire laser (MIRA, Coherent, emitting at 800 nm, repetition rate 80 MHz, 100 femtosecond (fs) pulses, 2 W average output power) was used for generating optical injection. A set of two half-wave plates

and polarizing beam splitters were used to split and attenuate the beam to obtain the desired power at the focus of the objective, and to provide an output for a spectrum analyzer to monitor the mode-locked output. The beam was expanded using a $\times 6$ telescope to overfill the back aperture of a $\times 60$ objective lens (Nikon) of 0.8 numerical aperture, to obtain a near-diffraction-limited sub-micron spot at the focus. The beam was directed into a microscope (Eclipse Ti, Nikon), with a high reflecting mirror for 800 nm as shown, to direct the beam to the objective and split the laser beam from the image for viewing on the CCD camera (DFK41BU02, The Imaging Source). The transmission of the objective lens was measured using a ‘dual objective’ method [48], allowing the optical power at the focus to be calculated from the power measured at the back aperture, which was set to 90 mW at the focus for the data presented in the results section. This power was chosen as a physical response (bubble formation, followed by cell “blebbing”) could be observed at higher powers, which is typically associated with permanent membrane damage and subsequent cell death.

The optical and fluid flow parameters were chosen such to mimic as closely as possible the situation of successful photoporation of adherent cells in a Petri dish, where typically between one and three laser doses of a few 10’s ms would be delivered for generating optical injection [13,15,17]. A shutter (LST200-IR, nmLaser Products) was incorporated into the beam path to continually pulse the beam, to deliver a stream of 4 ms (125 Hz square wave trigger signal) laser doses to the cells as they traversed the beam. The flow rate of $1100 \mu\text{m s}^{-1}$ was chosen such that a typical cell of 20 μm diameter would receive two or three 4 ms laser doses as it flowed through the focal spot, depending on its relative phase with the shutter. The laser dose duration was such to restrict each dose to within a few micrometers on the cell surface, whilst being within an order of magnitude of that used in photoporation of adherent cells. The fluence of each laser dose would therefore be sufficient to generate the required free-electron plasma for pore formation [26], with the physical mechanism matching that for photoporating adherent cells, and for similar optical powers (90 mW). Thus, it is the optical parameters required for successful photoporation rather than the fluid flow velocity that limits the throughput in this microfluidic optical injection system.

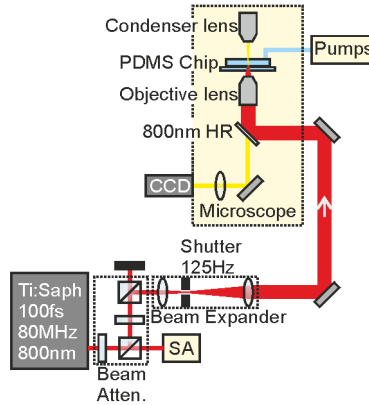


Fig. 3. Schematic of the optical setup, showing the Ti: Sapphire laser, power attenuators (2x half-wave plate and polarizing beam-splitter), spectrum analyzer (SA), beam expanding telescope, and the microscope containing: a high-NA objective lens for focusing the optical injection beam, and condenser lens, 800 nm high reflector (HR) and CCD camera. The PDMS microfluidic chip sits on the microscope stage and the fluid pumps are housed on adjacent raised platforms.

5. Microfluidic optical injection

The chip and fluidics were sterilized before each experiment, with the PDMS chip being used once only and autoclaved before use. The piping, syringes and connects were flushed with 70% ethanol, rinsed with filter-sterilized deionized water and finally dried with filtered air

using the peristaltic pump. The chip, piping and syringes were then filled, from the outlet end to minimize bubble formation, with filtered Opti-MEM® solution also containing the PI to be injected optically. The cell injection ports were sealed during filling procedure using Nescofilm (VWR) such that the outlet port had a higher fluid level than the inlet. This ensured that when inserting the cell sample, a back flow occurred to ensure the cells did not flow to the collection port before the system was stabilized and beam turned on. Once filled, the fluid switching valves were used to isolate the fluid pipes necessary for hydrodynamic focusing from the peristaltic pump and associated cleaning pipes, producing a closed fluid system.

The accompanying video demonstrates the flowing of cells in the microfluidic chip for optical injection, and four still images from this are shown in Fig. 4. HEK293 cells were inserted into the chip via the micro-centrifuge tube ‘insertion port’. A 20 μl cell sample was pipetted into the port and allowed several minutes for it to settle onto the coverslip (base of the channel), as monitored on the CCD camera. Once settled, the syringe pumps were turned on, generating a stable hydrodynamic focused flow of cells, close to the bottom of the channel. In effect, the system is close to 2D hydrodynamic focusing, where the combination of gravity and 1D hydrodynamic focusing confines the cells in both vertical and horizontal position in the channel. The focused laser beam was positioned approximately two channel widths (300 μm) downstream from the focusing junction, in the centre of the cell stream and raised 6 μm from the base of the channel (coverslip), which was found to be most optimal for hitting the cells. Cells would then come to rest under the ‘collection port,’ due to the considerably larger cross section and hence slower flow channel in this region.

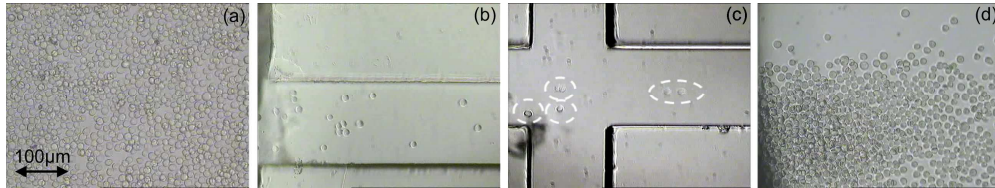


Fig. 4. ([Media 1](#)) Frames from the accompanying video, from within the PDMS microfluidic chip shown schematically in Fig. 1(b). (a) Sample injection port after the insertion of cells into the chip. (b) Cells flowing from left to right out of the injection reservoir and towards (c) the hydrodynamic focusing junction, where cells (circled) can be seen flowing single file down the center of the channel after the junction. The focused femtosecond laser beam for optical injection was situated 300 μm downstream of the junction. (d) Cell collection port after 10 minutes showing several hundred optically injected cells that have come to rest due to the drop in flow velocity in this region of the chip.

After flowing the cells for typically 10 minutes, or once approximately 500 cells had passed through the beam, the syringe pumps were stopped, the collection port opened, and the cells beneath this port removed from the chip using a pipette. We estimate that approximately 80% of the cells could be successfully removed and collected using this method, losses mainly due to cells remaining in the pipette tip rather than in the chip itself. The contamination from un-porated cells coming from the rest of the chip is negligible during the collection process. Upon collection, the chip was removed, the piping rinsed and sterilized, and the system was ready for a new chip and cell sample. Following the removal of the optically injected cells, the control samples were collected from the injection port. The contamination from optically injected cells was observed to be absolutely negligible.

6. Efficiency of injection and cell viability

Upon laser treatment, cells were collected from the chip collection port (for treated cells) and loading port (for untreated cells) into two separate micro-centrifuge tubes both containing 1 μM of CAM in 250 μl of conditioned DMEM. Cells were incubated (37°C, 5% CO₂) in two separated wells of 96-well Cell Culture Insert Plates (Millipore) for 15 minutes to stain cells with CAM, as well as allowing time for the cells to settle to the bottom of the wells. Next, 200 μl of the surrounding solution was gently removed from both the wells. During this process, extra care was taken in order not to remove any of the cells deposited at the bottom of the

plates. Following this, 200 μ l of conditioned DMEM was added so as to dilute the CAM to negligible levels and halt the uptake by the cells. The cells were incubated for a further 1 hour before examining PI (uptake due to optical injection and/or cell death) and CAM (indicating the viable cells) fluorescence of both the treated and untreated (control) cells under a fluorescent microscope.

Counts of typically 150 cells per experimental run were conducted for the two fluorophores. The cell samples were checked for: a) total number of cells; b) number of PI fluorescing cells; c) number of cells exhibiting both PI and CAM fluorescence. A typical image of the HEK293 cells is shown in Fig. 5, showing the brightfield, PI and CAM fluorescence images. These images were obtained 24 hours post optical injection, with cells exhibiting healthy growth, division, continued viability and PI fluorescence.

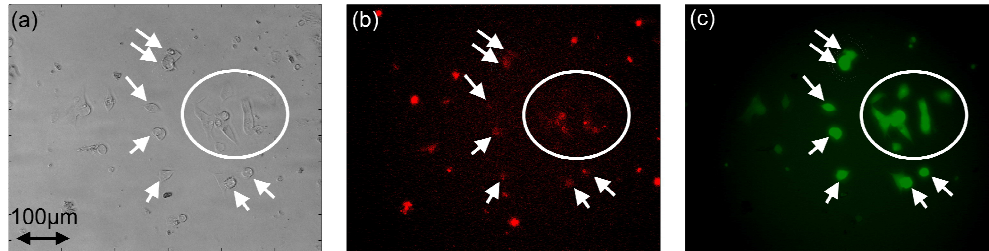


Fig. 5. Collected cells 24 hours after microfluidic photoporation, including viable optically injected cells (arrowed and circled). (a) Bright field microscope image showing cell attachment to the base of the well plate. (b) The same cells exhibiting varying levels of PI fluorescence. Strongly red fluorescing cells have taken up large quantities of PI indicating permanently compromised dead or dying cells. Weakly fluorescing red cells are optically injected. (c) Fluorescence of CAM showing the viable cells in this field of view. The combination of PI fluorescence in (b) and CAM indicates a cell that has been optically injected with PI and has remained viable (arrowed and circled).

Cell counts were conducted on the collected samples after 1.5 hours in the incubator. Figure 6 shows the success rate of optically injecting HEK293 cells using this microfluidic approach. Uptake of purely PI was found to be $42 \pm 8\%$ compared to a control of $4 \pm 2\%$. Taking into account CAM, the proportion of cells that exhibited both fluorescence of PI and a strong CAM signal, i.e. cells that are optically injected and viable was $28 \pm 4\%$, compared to a negligible control. These values are comparable to those obtained in Petri dish experiments, demonstrating that the technique is successful in optically injecting cells with an order of magnitude increase in throughput compared to a manual approach.

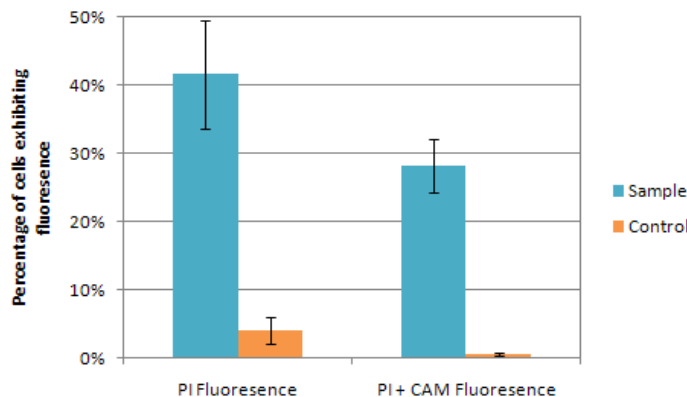


Fig. 6. Optical injection efficiencies for HEK293 cells in a microfluidic flow. The percentage of cells exhibiting fluorescence of PI and those that exhibit both PI and CAM is plotted here against those observed in the control samples. Cells exhibiting both PI and CAM are viable after optical injection of PI. Data was obtained 1.5 hours after collection from the chip and error bars are the standard error in the mean of three experimental runs.

7. Conclusion

A photoporation system has been presented, where a microfluidic chip is utilized to deliver cells to a focused fs laser, producing continuous and automated optical injection of a membrane impermeable substance to the cytoplasm of the cell. Throughputs of the order of 1 cell per sec were obtained, enabling several thousand viable injected cells per hour and as such is the first demonstration of fs-enabled optical injection on this scale. The injection efficiency and viability of the HEK293 mammalian cell line was confirmed using propidium iodide and calcein AM respectively. The injection efficiency using this technique was $42 \pm 8\%$ compared to a control of $4 \pm 2\%$ at a laser power at the focus of 90 mW. Taking into account the requirement for viable cells after injection, the viable injection efficiency was found to be $28 \pm 4\%$, for cells exhibited both propidium iodide and calcein AM fluorescence. One could expect these numbers to increase with better positioning of the height of cells through two dimensional hydrodynamic focusing [49] and thus improved targeting of the membrane, or by means of a “diffraction-free” Bessel beam [17]. Flow velocities of $1100 \pm 100 \mu\text{ms}^{-1}$ were used, which in combination with a continuous stream of 4 ms femtosecond laser doses, potentially lead to the creation of an array of two to three “photopores” across the cell as it traversed the beam, thus allowing uptake of the surrounding medium.

The work highlights the possibilities for optical injection as a realistic alternative to other injection techniques such as electroporation, microinjection, ballistic particle insertion (gene gun), or chemical or viral mediated methods. The advantages of microfluidics and fs optical injection are combined to provide a cell injection system with increased throughput, high injection efficiencies, high viability, with cheap, disposable, sterile microfluidic chips for a low (10^3 's μl) sample consumption.

Future developments could include the combination with on-chip functionality or other optical techniques, such as Raman [41] or fluorescence spectroscopy [40], or optical landscapes for active or passive sorting [43], before and/or after photoporation. Viability or injection efficiency measurements could be made on the chip and the sample purified, or by using multiple laser powers, cells could be injected or terminated in a sorting device. The combination of optical injection with on-chip cell culture could also be of particular interest. Immediate applications will be to apply the technique to the transfection of cells, including non adherent stem cells, through the insertion of plasmid DNA.

Acknowledgements

This work was supported by funds from the UK Engineering and Physical Sciences Research Council. KD is a Royal Society-Wolfson Merit Award Holder. The authors would like to thank David Stevenson and Maria Leilani Torres-Mapa for many useful discussions and support in the biological preparations. RFM and YA contributed equally to this work. FGM and KD contributed equally to this work.